RESEARCH ARTICLE

Solid particle erosion performance of micro-arc oxidation and electro spark deposition coated Ti6Al4V sheets

Doğan Acar*[1], Salim Levent Aktuğ[2], Kemal Korkmaz[2], Salih Durdu[3], Ömer Necati Cora[1]

[1]Karadeniz Technical University, Engineering Faculty, Department of Mechanical Engineering, Trabzon, Turkey
[2]Gebze Technical University, Engineering Faculty, Department of Materials Science and Engineering, Gebze, Turkey
[3]Giresun University, Engineering Faculty, Department of Industrial Engineering, Giresun, Turkey

Article Info	Abstract
	In this study, an aerospace-grade Ti6Al4V alloy was coated by micro-arc oxidation (MAO) and electro spark deposition (ESD) methods to investigate their effect on solid particle erosion performance. The surface morphology and mechanical properties of coatings were characterized by SEM and nanoindentation, respectively. Solid particle erosion performance of uncoated and coated Ti6Al4V alloy was investigated by using an in-house developed test system per ASTM G76-13 test standard. The effect of impact velocity (70 and 150 m/s) on erosive wear was examined using angular-shaped SiC erodent particles. The SEM analyses indicated the formation of cracks on coated surfaces after erosion tests. The MAO coatings' surface was rough and porous due to plasma chemical reactions on micro discharge channels. In addition, the nature of the ESD method resulted in deposits having rough surfaces owing to the rapid solidification of melted electrode and substrate materials under atmospheric conditions. Surface topography and crater depths were determined using a surface profilometer. Erosion rate was found to be increased with increasing impact velocity due to increased kinetic energy of erodent particles. Both MAO and ESD coated samples showed worse erosion performance compared to base Ti6Al4V material considering volumetric and gravimetric wear rates.

1. Introduction

Solid particle erosion is a dynamic process that results in material removal from a target surface due to the continuous impingement of erodent solid particles. It is a life-limiting phenomenon that is also an economic burden as many industries including aerospace, oil, and gas industry suffer from solid particle erosion [1, 2].

Micro-arc oxidation (MAO), also known as plasma electrolytic oxidation (PEO), combines electrochemical oxidation and high voltage spark. This is an effective technique to deposit various functional hard and porous ceramic coatings on the surfaces of valve metals such as Al, Mg, Ti, and their alloys [3, 4]. The MAO coatings produced on Ti and its alloys resulted in high hardness, high adhesion strength on the substrate, and excellent wear resistance [4, 5]. In another study, aluminum and aluminum-oxide-based duplex coatings were applied on Ti6Al4V alloy by using combined electro-spark deposition (ESD) and micro-arc oxidation (MAO) methods [18]. The ESD was carried out to accumulate an Al on Ti6Al4V alloy substrate at the first step. And then, an oxide-based layer was fabricated to improve mechanical and tribological properties of Ti6Al4V alloy by MAO process at the second step.

There are numerous studies on solid particle erosion of Ti6Al4V alloy [6–12]. Avcu et al. investigated the effect of impinging angle and erodent size effect to characterize the erosive behavior of Ti6Al4V [12]. They showed that Ti6Al4V presents a ductile material behavior and maximum erosion rate

obtained at 30° impingement angle. Also, elevated temperature erosion resistance of Ti6Al4V was investigated [6]. The erosion rate for Ti6Al4V was escalated with increasing temperature especially, between 600-800°C. Ti6Al4V coated with TiN, was used to investigate the porous coating structure on erosive behavior [7]. The effect of Cr layer thickness on erosive wear behavior of TiAlSiN/Cr coated Ti6Al4V was investigated in another study [13]. Furthermore, 21 nm thickness of the Cr layer is found to be optimum for excellent erosion resistance.

Krishna et al. investigated the ceramic coatings produced through the micro-arc oxidation method (MAO) [14]. It is stated that, in solid particle erosion performance, material removal is mostly related to unclosed discharge channels. In another study, Krishna et al. compared solid particle erosion behaviors of MAO coatings with hard-anodized coatings [15]. MAO coating showed better resistance than both hard-anodized coating and base alloy. However, the solid particle erosion rate is much more than MAO and base alloy.

Electro spark deposition (ESD) is another surface modification method to resist solid particle erosion. WC coating fabricated via ESD is explored for solid particle erosion performance and compared with WC-Co coatings' one by Roy [16]. Solid particle erosion resistance is enhanced by WC coatings and WC coatings showed a brittle response. However, there is no study on the solid particle erosion behavior of MAO and ESD coatings on Ti6Al4V alloy.

Corresponding Author: Doğan Acar
E-mail: dgnacar@ktu.edu.tr

In this study, the oxide- and metallic-based coatings were fabricated on Ti6Al4V alloy by MAO and ESD techniques, respectively. Then, the surface morphology and mechanical properties of both surfaces were investigated by SEM and nanoindentation test, respectively. The coatings fabricated on Ti6Al4V were investigated to reveal possible improvement in solid particle erosion performance.

2. Materials and methods

In the current study, Ti6Al4V alloy, (0.67 mm in thickness) manufactured per Aerospace Materials Standard (AMS4911F&H, ASTM B205-90 GRD5) was used as a base material. To enhance solid particle erosion response, Ti6Al4V was coated with micro-arc oxidation and electro spark deposition methods. Before coating processes, surfaces of Ti6Al4V to be coated were ground with sandpapers up to 1200 grit. After that, the surface of the titanium sheets was cleaned in an ultrasonic bath. Then, pure Al was deposited on a Ti6Al4V alloy through the ESD (electro spark deposition) process. A special ESD device was utilized at the first step. The ESD coating system was comprehensively described in detail in the authors' previous studies [17, 18]. The ESD process was performed using a hand-held applicator under constant temperature and in unipolar mode. In the system, the voltage dropped at the inter-electrode gap and the amount of electricity was kept constant. Besides ESD, Ti6Al4V substrates were coated by the MAO process. Bipolar impulses were used for the fabrication of the MAO oxide layer on the Ti6Al4V substrate as the second step. An alkaline electrolyte solution was prepared by mixing $NaAlO_2$ (#CAS: 1138-49-1 Sigma Aldrich) and KOH (#CAS: 1310-58-3 VWR Chemicals) in distilled water. A Ti6Al4V alloy and a stainless-steel container served as an anode and cathode, respectively. The treatment time was 10 min, and the current density was kept at 0.25 A/cm^2 through the MAO process. The schematic representations of the ESD and MAO coating procedures are shown in Fig. 1.
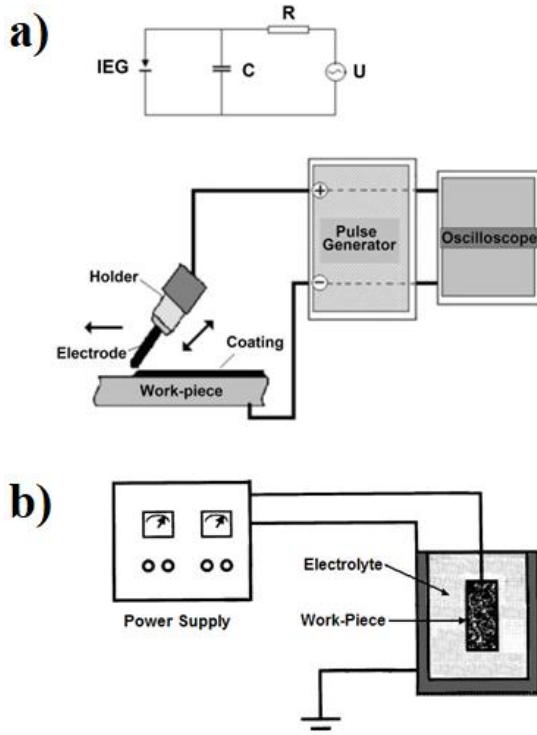
The surface morphologies of uncoated Ti6Al4V alloy, ESD, and MAO coatings were examined by SEM (Hitachi SU 1510) as seen in Figure 3. The average hardness and modulus of elasticity of the samples were determined by using the nanoindentation method.

Erosion test samples were prepared and were then tested per ASTM G76-13 test standard [19]. All samples were cut into dimensions of 25x25 mm^2. Base Ti6Al4V and Ti6Al4V samples coated with MAO and ESD were impacted at a 90° impact angle for two impact velocities (70 and 150 m/s). Angular-shaped SiC was used as an erodent particle. The average size in diameter of SiC particles was determined as 348 µm using Mastersizer (Malvern Panalytical Ins. Malvern, UK). SEM image of SiC particle is given in Figure 2-b. Erodent particle feed rate was set to 2.5 g/min and calibrated after three samples were tested. A convergent-divergent nozzle, its dimensions are given in Figure 2-c, was set to 10 mm stando-ff distance from test samples. Details of test parameters are given in Table 1. Impact velocity calibration of the SiC particles was carried out using the double-disk method [20]. Corresponding tank pressure values for 70 and 150 m/s impact velocities are determined as 1100 and 6630 mbar, respectively. Each test lasts 12 minutes, in total. The mass loss of the samples was measured after every 3 minutes of testing. All the erosion tests were performed using a solid particle erosion test system whose schematic is given in Figure 2-a [21]. After the tests, the eroded zone of each sample was scanned with a NanoFocus surface profilometer (NanoFocus AG, Oberhausen, Germany) to evaluate surface topology.
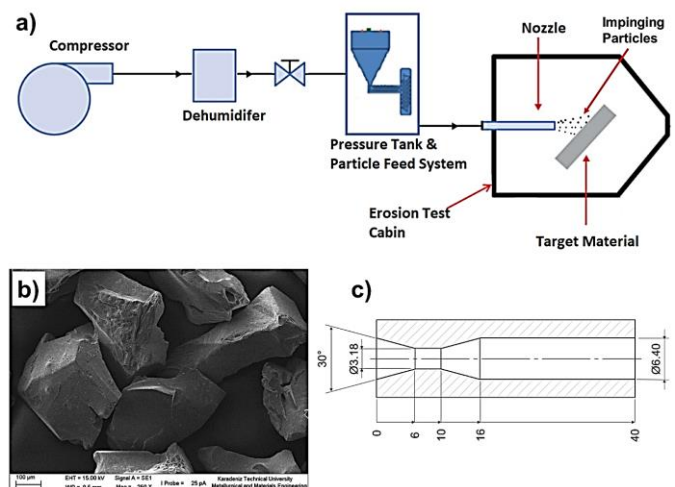

Figure 2. a) Schematic of the solid particle erosion test system, b) SEM image of SiC (348 µm) erodent particles and, c) Convergent-divergent nozzle, used in the test (dimensions are in mm.)

Figure 1. Schematic representations of coating systems, a) ESD device and b) MAO device [18]

Table 1. Erosion Test Parameters

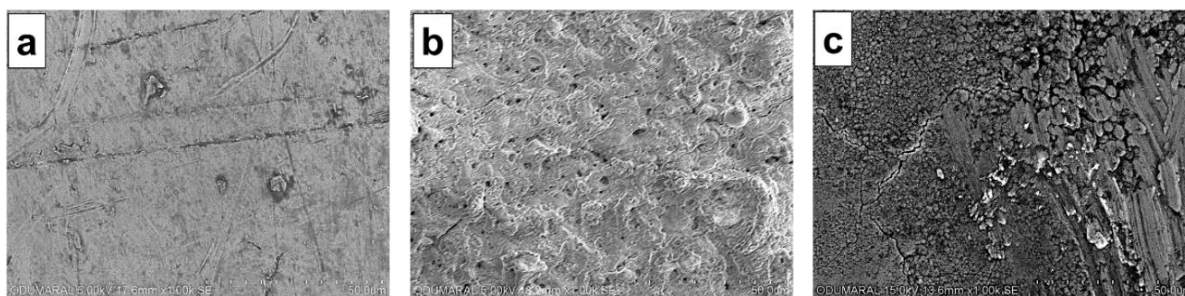|	Test Materials	Ti6Al4V	Ti6Al4V +MAO	Ti6Al4V +ESD
Test Parameters	Impact Velocity	70 - 150 m/s		
	Impact Angle	90°		
	Erodent Type	Silicon Carbide (SiC)		
	Erodent Size	348 µm		
	Nozzle Stand of Distance	10 mm		
	Test Standard	ASTM G76-13		

Figure 3. SEM images of sample surfaces, a) Ti6Al4V, b) Ti6Al4V+MAO, c) Ti6Al4V+ESD

3. Results and discussion

The surface morphologies of uncoated Ti6Al4V, MAO, and ESD coated samples were examined by scanning electron microscopy as shown in Figures 3-a, 3-b, and 3-c, respectively. The surface of uncoated Ti6Al4V alloy was smooth compared to MAO and ESD surfaces. Only, a few grinding traces were observed through the whole surface due to the grinding with sandpaper (Figure 3-a). However, the MAO-coated Ti6Al4V surfaces were porous and rough due to the presence of micro-discharge channels that occurred during the MAO process. Moreover, there are some cracks near the micro discharge channels owing to the rapid solidification of the electrolytes during the process (Figure 3-b). The ESD-coated Ti6Al4V surfaces were irregular and rough as shown in Figure 3-c. Besides, some cracks were observed on ESD coated Ti6Al4V alloy owing to rapid solidification of melted electrodes contacted to Ti6Al4V alloy under atmospheric conditions.

The hardness value has a critical role in the wear behavior of the materials. To evaluate the hardness and modulus of elasticity of MAO and ESD coated Ti6Al4V samples, nanoindentation tests were carried out on the coated samples as given in Figure 4. 10 mN load was applied to the samples at least 5 times for each coated sample. The hardness values of MAO and ESD coatings were approximately measured as 0.32 GPa and 2.20 GPa, respectively. Modulus of elasticity values of MAO and ESD coatings were measured as 4.2 GPa and 39.7 GPa, respectively. The hardness value of the coatings usually depends on phase structure and microstructure. The microstructure of MAO coating is not high enough whereas it contained oxide phases as shown in Figure 3-b. The microstructure of MAO coating contains some pores as well as brittle oxide phases as shown in Figure 3-b. Nevertheless, the ESD coating had a compact microstructure compared to the MAO surface as seen in Figure 3-c. It can be concluded that the microstructure of the coatings had critical importance on hardness. Thus, the MAO coating usually had a lower hardness value than that of the ESD coating.
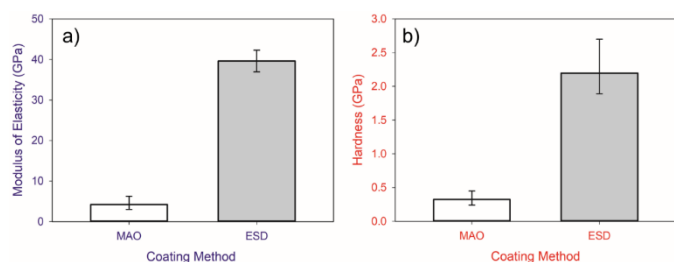

Figure 4. a) Modulus of elasticity and b) hardness values obtained from nanoindentation tests.

Mass loss measurements were carried out with a precision scale after every three minutes of erosion testing (in total 12 min. for a test sample) and were recorded. Calculated mass loss values of tested samples were depicted in Figure 5. Examining Figure 5, it is observed that Ti- MAO samples showed the worst erosion performance when the mass loss is considered. Besides, increasing impact velocity resulted in mass loss increase.
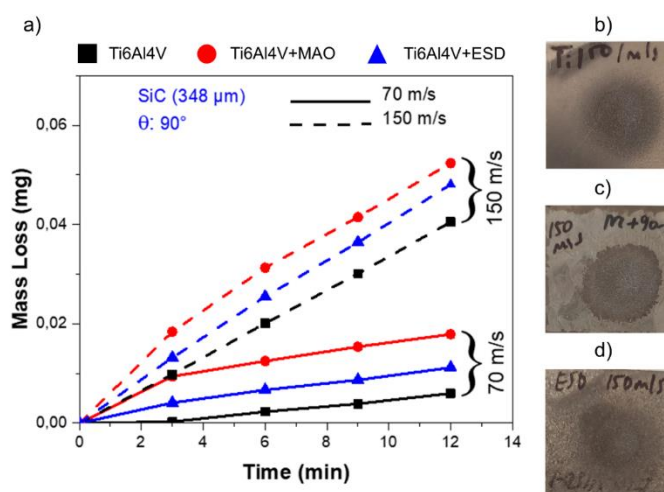

Figure 5. a) Variation of mass losses with time at different impact velocities, surface photographs of eroded tests samples, b) Ti6Al-4V, b) Ti6Al4V+MAO, c) Ti6Al4V+ESD

Eroded surfaces of Ti6Al4V, Ti6Al4V+MAO, and Ti6Al4V+ESD samples were scanned with a Nanofocus surface profilometer. Scanned surface images and corresponding surface topographies at 70 and 150 m/s are given in Figure 6. Scales on the right side of the topographies show that crater depths increase with increasing impact velocity. In Figure 6-b, c, brittle ruptures around the erosion zone were observed on the MAO surface. The reason for brittle ruptures on the MAO surface can be attributed to its chemical structure. Furthermore, the outer layer of the MAO surface is an amorphous structure because of the rapid solidification of electrolytes through the MAO process. Thus, the MAO surfaces can be brittle compared to uncoated Ti6Al4V and Ti6Al4V+ESD metal surfaces. As a result, the mass loss of the MAO surface is higher compared to those of Ti6Al4V and Ti6Al4V+ESD. Therefore, width-depth profiles from the cross-section in the deepest point of the craters that occurred on the eroded surface were extracted. After that, these width-depth profiles were overlaid on each other for different test samples for 70 and 150 m/s impact velocities (Figure 7). Increasing impact velocity from 70 m/s to 150 m/s increased the erosion depth by about six times. However, the crater widths for all tested samples, whether uncoated or coated, remain almost the same. As for volumetric erosion evaluation, the erosion trend is a slightly different from mass loss values.
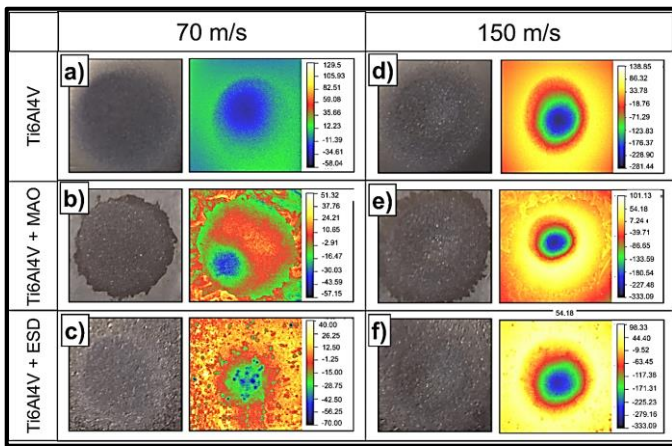
Figure 6. Surface topographies of tested samples at 70 m/s a) Ti6Al4V, b) Ti6Al4V +MAO, c) Ti6Al4V +ESD, and at 150 m/s d) Ti6Al4V, e) Ti6Al4V+MAO, f) Ti6Al4V+ESD (All the legends are in µm)

In this case, Ti6Al4V+ESD eroded more than both Ti6Al4V+MAO and Ti6Al4V. In any case, coated Ti6Al4V samples did not yield better erosion performance contrary to expectations. As a result, uncoated Ti6Al4V showed the best solid particle erosion performance when both volumetric and mass loss values are considered.
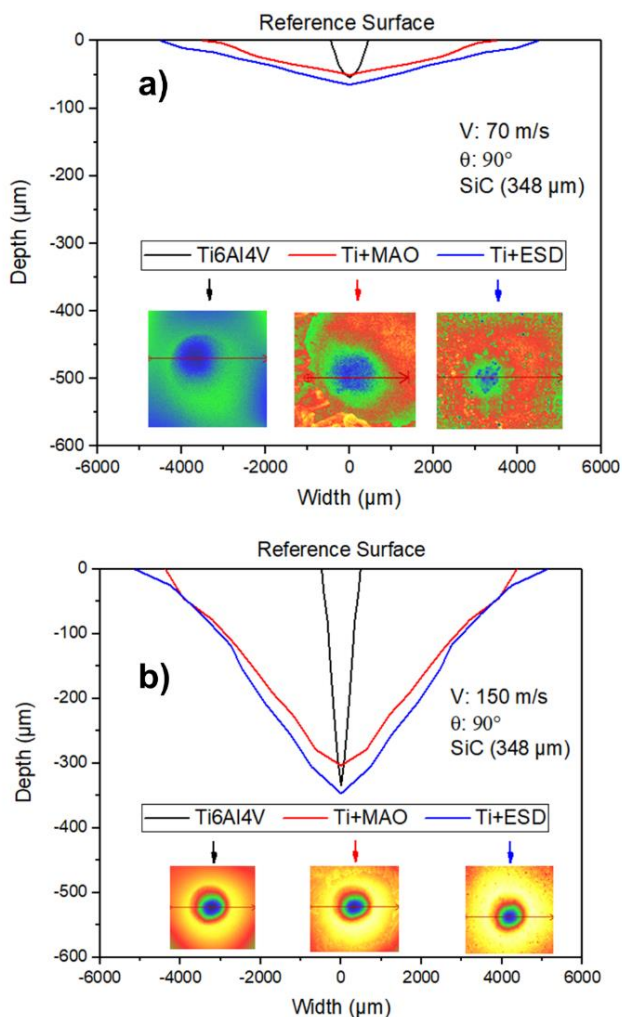

Figure 7. Cross-sectional erosion profile curves for eroded surfaces of the samples tested at their deepest point, a) 70 m/s, b) 150 m/s
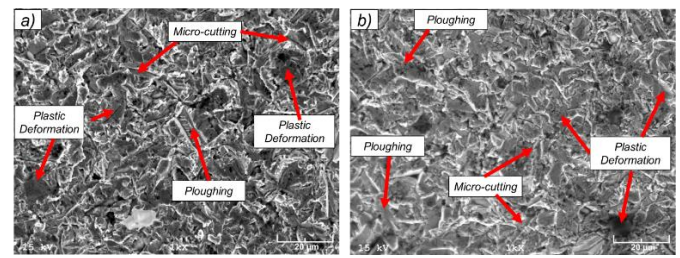

Figure 8. SEM images of tested samples subjected to solid particle erosion at 150 m/s impact velocity and 90° impinging angle, a) ESD, b) MAO

In Figure 8, scanning electron microscopy (SEM) images depicts observed the solid particle erosive wear mechanisms of both ESD and MAO samples at 150 m/s impact velocity and particle impingement angle at 90°. Ploughing and micro-cutting are the dominant erosive wear mechanism for both coating types. Plastic deformation erosive wear mechanism is also observed.

4. Conclusions

In this study, Ti6Al4V was coated with two different coatings, namely an oxide layer using micro-arc oxidation (MAO) and aluminum employing electro spark deposition (ESD) methods. The coated and uncoated Ti6Al4V samples were subjected to solid particle erosion tests at 70 and 150 m/s impinging particle velocities and 90° impact angle using SiC erodent particles. SEM observations on the samples revealed a porous coatings structure and cracks on the surface of Ti6Al4V+MAO samples before erosion tests. Similarly, a rough surface along with cracks was observed on the Ti6Al4V+ESD samples. In erosion tests, increasing impact velocity led to an increased amount of erosion, as expected. Nevertheless, the coated samples performed worse compared to uncoated Ti6Al4V. Even though it needs further investigation, this can be attributed to the insufficient bonding between the coating and substrate as well as the high discrepancy between the hardness values of base metal and the coatings. Considering the mass loss values, Ti6Al4V+MAO samples showed the worst erosion performance at both impact velocities. On the other hand, Ti6Al4V+ESD samples were eroded more compared to Ti6Al4V and Ti6Al4V+MAO samples when the volumetric loss is taken into consideration.

The effect of impact angle and coating procedure parameters on the erosion performance of the coating can be investigated as a future study.

Author contributions

Doğan Acar: Conceptualization, Data curation, Investigation, Roles/Writing - original draft

Salim Levent Aktuğ: Investigation, Methodology, Visualization

Kemal Korkmaz: Investigation, Methodology, Visualization.

Salih Durdu: Supervision, Validation, Writing - review & editing

Ömer Necati Cora: Supervision, Formal analysis, Writing - review & editing.

References

1. Parsi, M., Najmi, K., Najafifard, F., Hassani, S., McLaury, B.S., Shirazi, S.A., A comprehensive review of solid

particle erosion modeling for oil and gas wells and pipelines applications, J. Nat. Gas Sci. Eng. 21, **2014**, 850–873

2. Schmitt, G.F., Liquid and Solid Particle Erosion, Technical Report, **1979**

3. Durdu, S., Deniz, Ö.F., Kutbay, I., Usta, M., Characterization and formation of hydroxyapatite on Ti6Al4V coated by plasma electrolytic oxidation, J. Alloys Compd, **2013**, 551, 422–429

4. Durdu, S., Bayramoğlu, S., Demirtaş, A., Usta, M., Üçışık, A.H., Characterization of AZ31 Mg Alloy coated by plasma electrolytic oxidation, Vacuum, **2013**, 88,130–133

5. Yerokhin, A.L., Nie, X., Leyland, A., Matthews, A., Dowey, S.J., Plasma electrolysis for surface engineering, Surf. Coatings Technol, **1999**, 122, 73–93

6. Zhou, J., Bahadur, S., Erosion-corrosion of Ti-6Al-4V in elevated temperature air environment, Wear, **1995**, 186–187, 332–339

7. Proudhon, H., Savkova, J., Basseville, S., Guipont, V., Jeandin, M., Cailletaud, G., Experimental and numerical wear studies of porous Reactive Plasma Sprayed Ti–6Al–4V/TiN composite coating, Wear, **2014**, 311, 159–166

8. Kumar, N., Shukla, M., Finite element analysis of multi-particle impact on erosion in abrasive water jet machining of titanium alloy, J. Comput. Appl. Math., 2012, 236, 4600–4610

9. Kamkar, N., Bridier, F., Bocher, P., Jedrzejowski, P., Water droplet erosion mechanisms in rolled Ti–6Al–4V, Wear, **2013**, 301, 442–448

10. Farina, I., Fabbrocino, F., Colangelo, F., Feo, L., Fraternali, F., Surface roughness effects on the reinforcement of cement mortars through 3D printed metallic fibers, Compos. Part B Eng., **2016**, 99, 305–311

11. Takaffoli, M., Papini, M., Material deformation and removal due to single particle impacts on ductile materials using smoothed particle hydrodynamics, Wear, 2012, 274–275, 50–59

12. Avcu, E., Fidan, S., Yildiran, Y., Sinmazçelik, T., Solid particle erosion behaviour of Ti6Al4V alloy, Tribol. - Mater. Surfaces Interfaces, 2013, 7, 201–210

13. Gu, J., Li, L., Ai, M., Xu, Y., Xu, Y., Li, G., Deng, D., Peng, H., Luo, S., Zhang, P., Improvement of solid particle erosion and corrosion resistance using TiAlSiN/Cr multilayer coatings, Surf. Coatings Technol., **2020**, 402, 126270

14. Rama Krishna, L. Somaraju, K.R.C., Sundararajan, G., The tribological performance of ultra-hard ceramic composite coatings obtained through microarc oxidation, Surf. Coatings Technol., **2003**, 163–164, 484–490

15. Krishna, L.R., Purnima, A.S., Sundararajan, G., A comparative study of tribological behavior of microarc oxidation and hard-anodized coatings, Wear, **2006**, 261, 1095–1101

16. Roy, M., Solid Particle Erosion Behavior of WC Coating Obtained by Electrospark Technique and Detonation Spraying, Tribol. Trans., **2014**, 57, 1028–1036

17. Ribalko, A.V., Korkmaz, K., Sahin, O., Intensification of the anodic erosion in electrospark alloying by the employment of pulse group, Surf. Coatings Technol., 2008, 202, 3591–3599

18. Durdu, S., Aktuğ, S.L., Korkmaz, K., Characterization and mechanical properties of the duplex coatings produced on steel by electro-spark deposition and micro-arc oxidation, Surf. Coatings Technol., **2013**, 236, 303–308

19. ASTM G76-07, Standard Test Method for Conducting Erosion Tests by Solid Particle Impingement Using Gas Jets, West Conshohocken, PA, **2013**

20. Ruff, A.W., Ives, L.K., Measurement of solid particle velocity in erosive wear, Wear, **1975**, 35, 195–199

21. Acar, D., Meriç, D., Sofuoğlu, H., Gümrük, R., Cora, Ö.N., Gedikli, H., Helikopter Pali Aşınma Kalkanında Meydana Gelen Katı Parçacık Erozyonunun İncelenmesi İçin Bir Test Düzeneği Tasarım Ve İmalatı, in: VI. Ulus. Havacılık Ve Uzay Konf., Kocaeli, Türkiye, **2016**,1–13